CXCR6 Induces Prostate Cancer Progression by the AKT/Mammalian Target of Rapamycin Signaling Pathway

Jianhua Wang,[1,2] Yi Lu,[4] Jingchen Wang,[2] Alisa E. Koch,[3] Jian Zhang,[4] and Russell S. Taichman[2]

[1]Shanghai Jiao-Tong University School of Medicine, Institute of Medical Sciences, Shanghai, P. R. China; [2]Department of Periodontics and Oral Medicine, University of Michigan School of Dentistry and [3]VA Medical Center and Department of Medicine, University of Michigan Medical School, Ann Arbor, Michigan; and [4]Department of Medicine, University of Pittsburgh, Pittsburgh, Pennsylvania

Abstract

Previous studies show that the chemokine CXCL16 and its receptor CXCR6 are likely to contribute to prostate cancer (PCa). In this investigation, the role of the CXCR6 receptor in PCa was further explored. CXCR6 protein expression was examined using high-density tissue microarrays and immunohistochemistry. Expression of CXCR6 showed strong epithelial staining that correlated with Gleason score. *In vitro* and *in vivo* studies in PCa cell lines suggested that alterations in CXCR6 expression were associated with invasive activities and tumor growth. In addition, CXCR6 expression was able to regulate expression of the proangiogenic factors interleukin (IL)-8 or vascular endothelial growth factor (VEGF), which are likely to participate in the regulation of tumor angiogenesis. Finally, we found that CXCL16 signaling induced the activation of Akt, p70S6K, and eukaryotic initiation factor 4E binding protein 1 included in mammalian target of rapamycin (mTOR) pathways, which are located downstream of Akt. Furthermore, rapamycin not only drastically inhibited CXCL16-induced PCa cell invasion and growth but reduced secretion of IL-8 or VEGF levels and inhibited expression of other CXCR6 targets including CD44 and matrix metalloproteinase 3 in PCa cells. Together, our data shows for the first time that the CXCR6/AKT/mTOR pathway plays a central role in the development of PCa. Blocking the CXCR6/AKT/mTOR signaling pathway may prove beneficial to prevent metastasis and provide a more effective therapeutic strategy for PCa. [Cancer Res 2008;68(24):10367–76]

Introduction

The high mortality rate of prostate cancer (PCa) is closely associated with the spread of malignant cells to various tissues in the body including bone. Intriguingly, evidence suggests that chemokines are likely to play a crucial role in mediating the continuous series of events leading to tumor growth and metastasis (1–3). Therefore, it is important to understand chemokine signaling in PCa to get a better understanding of the underlying mechanisms leading to tumor invasion and metastasis, and to develop prognostic and therapeutic strategies in this disease.

During the events in which PCa metastasizes to bone marrow, the cancer cells must first migrate out of the prostate, adhere to the endothelial marrow cells, and subsequently extravasate and proliferate in the extravascular marrow spaces. All of these events are functionally similar to hematopoietic cells as they move in and out of the bone marrow, an event that seems to be largely regulated by chemokines (3, 4).

Chemokines are small proinflammatory chemoattractant cytokines that bind to G-protein–coupled seven-span transmembrane receptors that are major regulators of cellular trafficking. Based on the number and position of conserved cysteine residues near the NH_2 terminus, chemokines are classified by their structure into four groups, namely CC, CXC, C, and CX3C. Over the past several years, there is emerging evidence that multiple pairs of chemokines and their receptors play critical roles in cancer progression (5–7).

Our group and others have shown that CXCL12 and its receptor are critical elements in growth and metastasis of PCa to tissues that produce large quantities of CXCL12 (8, 9). More recently, we have shown that a second CXCL12 receptor, CXCR7/RDC1, also plays a central role in PCa metastasis and progression (10). However, blockade of the CXCR4 or CXCR7 receptor only partially blocks metastatic behavior *in vivo*. This suggests that other functional chemokine/chemokine receptor pairs may play an important role in tumor development (Supplementary Fig. S1).

Recently, CXCL16 was identified as a ligand for CXCR6, which is expressed by peripheral blood leukocytes (11). CXCL16 expression has been shown in a variety of tissues and cells including activated endothelial cells (12), Hodgkin's disease–derived tumor cells and tumor-associated macrophages in rectal cancer (13, 14). Additionally, CXCL16 has been shown to function as a potent and direct activator of nuclear factor-κB and induces κB-dependent proinflammatory gene transcription through heterotrimeric G proteins, PI3K, PDK-1, Akt, and IκB kinase (15). Moreover, CXCL16 increased cell-cell adhesion and induced the κB-dependent proliferation of human aortic smooth muscle cells, indicating that CXCL16 may play an important role in the development and progression of atherosclerotic vascular disease (15).

Although classified as a CXC chemokine, CXCL16 shares close structural similarities with fractalkine with a transmembrane domain, which makes this chemokine fundamentally different from the rest of CXC chemokines (16). CXCL16 is synthesized as a transmembrane molecule and transported to the cell surface. To exert its chemotactic activity, CXCL16 must be proteolytically cleaved and shed, a process that is regulated via a disintegrin and metalloproteinase 10 (16–18). Interestingly, although lacking an ELR motif in the chemokine domain, CXCL16 is proangiogenic. Similarly, Volin and colleagues (12) showed that fractalkine plays an important role in angiogenesis. The striking similarities between CXCL1 and both fractalkine and CXCL12 are likely to result in additive effects. Recent findings by Nakayama and colleagues (19)

Note: Supplementary data for this article are available at Cancer Research Online (http://cancerres.aacrjournals.org/).

Requests for reprints: Jianhua Wang, Shanghai Jiao-Tong University School of Medicine, Institute of Medical Sciences, Shanghai, 200025, P. R. China. E-mail: jianhuaw2007@gmail.com or Russell S. Taichman, Department of Periodontics and Oral Medicine, University of Michigan School of Dentistry, Ann Arbor, MI 48109. Phone: 734-764-9952; Fax: 734-763-5503; E-mail: rtaich@umich.edu.

doi:10.1158/0008-5472.CAN-08-2780

showed consistent expression of CXCL16 in tissues enriched with plasma cells, such as the bone marrow. This suggests that plasma cells are likely to be recruited to the bone marrow and other target tissues via CXCR6 (20). Interestingly, CXCR6 has subsequently been shown to be present in prostate tissues and in the marrow (19, 21). Through a cytokine antibody array, Lu and colleagues (5) reported that CXCL16 protein production was increased in aggressive PCa cells compared with the less-aggressive PCa cells or benign prostate cells. These observations raise the possibility that CXCL16/CXCR6 interactions may be important for PCa invasion and metastasis, as was shown for CXCL12/CXCR4 (7).

In this study, the role of CXCL16/CXCR6 chemokine axis in PCa progression was further explored. The results suggest that alterations of CXCR6 expression are associated with invasive growth and angiogenic activities of PCa cells. Our data shows for the first time that the CXCR6/AKT/mammalian target of rapamycin (mTOR) pathway plays a central role in the development of PCa. Therefore, blocking the CXCR6/AKT/mTOR signaling pathway is likely to have an antimetastatic effect, which may be beneficial in development of a more effective therapeutic strategy for PCa.

Materials and Methods

Cell cultures. The PC-3 cell line was originally isolated from a vertebral metastasis, the metastatic subline LNCaP C4-2B cells (called C4-2B cells) were originally isolated from a lymph node of a PCa patient with disseminated bone and lymph node involvement. PCa cell lines were passaged and grown to confluence over 5 d. For the production of PCa cell conditioned medium (CM), the cells were replated at 2.0×10^4 cells/cm^2 into 24-well tissue culture plates and incubated in growth medium (RPMI 1640 with 10% FCS and antibiotics; Invitrogen Corp.). After confluence, the cells were washed with PBS and the growth medium replaced and incubated for an additional 96 h. The CM were collected and frozen after passage through a 0.22-μmol/L filter. Human dermal microvascular endothelial cells (HDMEC) were grown as previously described (22).

Western blot analyses. PCa cells were cultured to confluence, washed, and then serum-starved in RPMI with 0.1% bovine serum albumin (BSA) for 24 h. Stimulation of the cells was performed with 100 ng/mL CXCL16 (R&D Systems). At selected time points, the cells were lysed in ice-cold radioimmunoprecipitation assay (RIPA) buffer (50 mmol/L Tris-HCl, 1% NP40, 120 mmol/L NaCl, 1 mmol/L EDTA, 25 mmol/L NaF, 40 mmol/L β-glycerol phosphate, 0.1 mmol/L sodium orthovanadate, 0.5 mmol/L phenylmethylsulfonyl fluoride, and 1.0% mammalian protease inhibitor cocktail; Sigma). Protein concentrations were determined from cell lysates clarified by centrifugation at 14,000 rpm for 10 min (Bio-Rad Laboratories). Normalized lysates (30 μg) were resuspended in loading buffer and were electrophoresed on 10% polyacyrlamide gels under reducing conditions and transferred to polyvinylidene difluoride membranes. For detection of CD44 and matrix metalloproteinase (MMP)-2, 3, 9 (Santa Cruz Biotech, Inc.), the membranes were either blocked in 3% BSA in PBS-0.1% Tween 20, and a rabbit anti-human monoclonal antibody (1 μg/mL; 1:1,000; Abcam, Inc.) or a mouse anti-human monoclonal antibody (1 μg/mL; 1:1,000; Sigma Corp.) were used in conjunction with anti-species conjugated horseradish peroxidase (HRP; 1:1,000; Upstate) and detected by chemiluminescence (Amersham Pharmacia, Inc.). AKT, p70S6K, and 4E-BP1 detection were similarly performed in 5% dry milk in PBS-0.1% Tween 20 with a rabbit monoclonal reactive to dually phospho-AKT (Ser473) p70S6K (Thr421/Ser424) and p4E-BP1 (Thr37/46), and total AKT, p70S6K, and 4E-BP1 (Cell Signaling Technology).

Construction of lentiviral vectors. For siRNA knockdown of CXCR6, the iLenti siRNA vector was purchased from Applied Biological Materials, Inc. (ABM), designed with convergent Pol III promoters that drive the transcription of target siRNA from opposite directions. Briefly, 5 μg of each lentiviral vector and 2.5 μg of each packaging vector were cotransfected in 293T cells by using Lentifectin (ABM). Supernatants were collected 36 to 48 h after transfection, filtered through a 0.4-μm filter, and used directly to infect tumor cells. Two rounds of infection 8 h apart were usually sufficient to infect >90% of cells. Transduced cells were selected in 500 μg/mL G418 (Invitrogen) for 1 wk, and cells with high green fluorescent protein levels were then isolated by fluorescence-activated cell sorting (FACS). Control cells were transduced with lenti-β-gal vector or with the empty vector and similarly sorted. The RNA interference CXCR6 (CXCR6 siRNA) target sequences:

1. 5′-TGCTATTCAGTCATAATCAAAACACTGCT-3′(628).
2. 5′-TTCGAGAAGCTGCTCTGGAATTTGCAAGT-3′(1043).
3. 5′-ACACTCTGGCTGGTTTGGAATGCTTCTTC-3′(1146).
4. 5′-CCAGGGACTATGAATGGGCAAAACTGAAT-3′(1587).

For construction of full-length CXCR6 expressing vector, ∼1.1-kilobase hCXCR6 cDNA was isolated by reverse transcription-PCR from total RNA extracted from PC3 cells. The forward and reverse primers were 5′-CCGGTCTAGAACCATGGCAGAGCATGATTACC-3′ (position: 79–100) and 5′-AGTAGGATCCCTATAACTGGAACATGCTGGTGGC-3′ (position: 1111–1087), respectively. The hCXCR6 cDNA contained the open reading frame of hCXCR6 was cloned to promoter specific lentiviral expression vector (ABM). The construction was verified by sequencing. The experimental protocol for transfection of the lentiviral expression vector in tumor cells was performed as described above.

Tissue microarrays and immunohistochemical staining. High-density tissue microarrays were constructed by US Biomax, Inc. with clinical samples obtained from a cohort of 48 patients. Tumors were graded using the Gleason grading system and examined to identify areas of benign prostate, PCa, and bone metastases. The formalin-fixed, paraffin-embedded tissues were dewaxed and placed in a pressure cooker containing 0.01 mol/L buffered sodium citrate solution (pH 6.0), boiled, and chilled to room temperature for antigen retrieval. The slides were then incubated for 1 h at room temperature with anti-human CXCR6 antibody (Novus Biologicals). MBA171 (IgG2a; Clone 44708.111; R&D Systems) was used as a negative control. Vectastain ABC-AP substrate kit (Vector Laboratories) was used for signal detection and Harris hematoxylin was used as a counterstain.

Cell invasion. Cell invasion was examined using a reconstituted extracellular matrix membrane (BD Biosciences). Test cells were placed in the upper chamber (1×10^5 cells per well) in serum-free medium, and 100 ng/mL CXCL16 was added to the bottom chambers. Invasion into the matrix after 48 h was determined by removal of the invasion chambers and 40 μL of 3-(4,5-dimethylthiazol-2-yl)-2,5-diphenyltetrazolium bromide (MTT; 5 mg/mL; Sigma) was added to the top well and 80 μL of MTT into the bottom well, and further incubated for 4 h at 37°C. After complete removal of the residual cells or medium, the purple residues attached to the bottom or top chambers were released with 1 mL isopropanol (Sigma). The invasion chambers were rocked for 30 min at a medium speed and then 100 μL from each well transferred into 96 wells and read on a multiwell scanning spectrophotometer (Molecular Devices Corp.) at OD_{450}.

Flow cytometry. For surface chemokine receptor detection, 2×10^5 cells were incubated at 2°C to 8°C for 40 min with nonspecific isotype-matched controls, mouse to human IgG (BD Biosciences), and 20 μg/mL of each of the following murine monoclonal antibodies: anti-human CXCR6 (R&D Systems; FAB699P). The mouse primary antibodies were then detected by incubating the cells at 25°C for 45 min with phycoerythrin. The cells were washed twice with PBS, resuspended and fixed in 1% (w/v) paraformaldehyde for analysis. Ten thousands cells from each sample were evaluated for fluorescence detection using FACScan (Becton Dickinson), and the data were analyzed with CellQuest software (Becton Dickinson).

ELISA. Antibody sandwich ELISAs were used to evaluate interleukin (IL)-8, and vascular endothelial growth factor (VEGF) levels in the PCa cell CM (R&D Systems) as previously described (22).

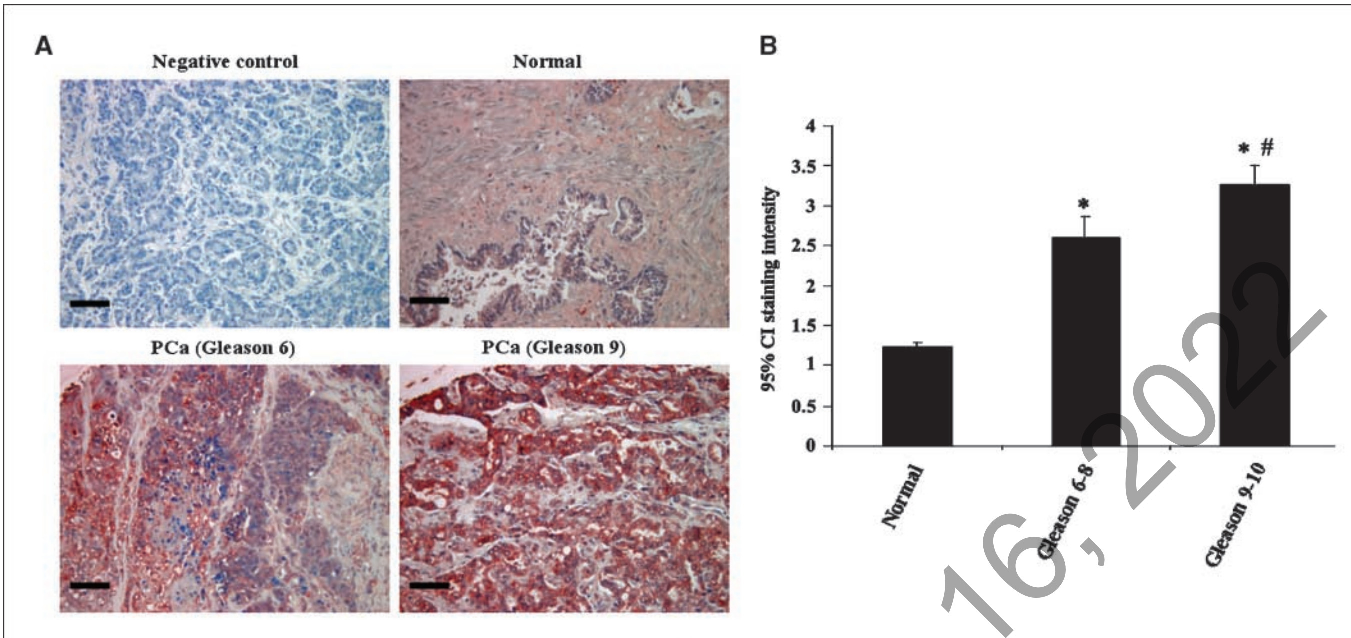

Figure 1. CXCR6 expression is correlated with human PCa development. *A,* the expression of CXCR6 in human PCa. Formalin-fixed paraffin-embedded tissues were incubated overnight at room temperature with anti-human CXCR6 antibody. MBA171 (IgG2a) was used as a negative control. Representative micrographs were taken at an original magnification ×20; *black bars,* 100 μmol/L. *B,* quantitative histologic evaluation of CXCR6 expression in PCa progression. CXCR6 expression intensity was scored on a four point scale as either negative (1), weak (2), moderate (3), or strong (4). Mean expression scores multiplied by percent positive cells in the field (Quick's combined score system) are presented for normal and localized PCa cases in a graphical format using error bars with 95% confidence intervals (*CI*). Statistically significant differences were noted between normal (n = 13) and PCa (Gleason, 6–8; n = 37) or PCa (Gleason, 9–10; n = 30), P < 0.001 (*), and between PCa (Gleason, 6–8) and PCa (Gleason, 9–10), #, P < 0.01 (ANOVA).

Angiogenesis antibody arrays. The expression of 19 cytokines was evaluated using Angiogenesis antibody arrays (Panomics). The membranes were exposed to blocking buffer for 1 h at 25°C, and incubated with CM or control medium up to 2 h at 25°C. After washing thrice, the arrays were processed with biotin-conjugated angiogenesis antibody mix and strepavidin-HRP conjugate according to the manufacturer protocol.

Endothelial sprout formation assays. Growth factor–reduced basement membranes were placed into 4-chamber slides (Matrigel; 125 μL/chamber; BD Biosciences), and 0.8 × 10^4 endothelial cells were added on top. The chambers were incubated at 37°C for 24 h. After incubation, the slides were fixed with methanol and stained with Diff-Quick solution II (Sigma). The slides were examined, and the sprouts were counted from 5 random fields using a microscope (×200). For coculture assays, 500 μL of the PCa CM or control was added daily to culture endothelial cells.

Subcutaneous tumor growth. All experimental animal procedures were performed in compliance of the institutional ethical requirements and approved by the University of Michigan Committee for the Use and Care of Animals. To evaluate tumor growth, s.c. tumors were established from the various transfectants by resuspending 2 × 10^6 PCa cells in growth factor–reduced Matrigel. Male 5- to 7-wk-old severe combined immunodeficient (SCID) mice (CB.17.SCID; Taconic) were anesthetized with isofluorane inhalation. After shaving and cleaning the skin, s.c. injections using a 27G needle were used to establish the tumors. The animals were monitored daily, and tumor volumes evaluated every 6 d starting at day 10. After 36 d, the animals were sacrificed, the tumors were weighed, measured, and prepared for histology.

Immunohistochemistry. For histologic evaluation of the tumor tissues, representative tumor tissues were fixed in formalin and embedded in paraffin. In addition, tumor tissues were also embedded in ornithine carbamyl transferase compound (Sakura Finetek) and stored at −80°C. For immunostaining with von Willebrand factor (Factor VIII–related antigen), tissue sections were blocked with Sniper for 5 min, and incubated overnight at 4°C with 12.5 μg/mL rabbit anti-human von Willebrand factor antibody (Neo Markers) diluted in PBS. The sections were incubated with appropriate secondary antibodies for 30 min, followed by processing with a Lincoln Label 41 Detection System (Biocare Medical). The HRP-AEC Chromogen System (R&D Systems) or a solution of HSS-HRP and AEC chromogen in chromogen buffer were used to visualize bound antibodies. Nuclei were identified by 4′,6-diamidino-2-phenylindole (DAPI; Vector Laboratories). The numbers of stained microvessels were blindly counted in 10 random fields per implant at ×630 magnification. Four or five implants were analyzed per condition and for each time point. All images were generated on Zeiss LSM 510 meta confocal laser scanning microscope. For immunostaining with Ki-67 antigen (Abcam), PC3 and C4-2B cells were cultured in Lab-Tek II 4-chamber slides (Nalge Nunc International) at 5 × 10^4 cells per chamber. After 24 h, the cells were incubated with PBS or CXCL16 (100 ng/mL) or rapamycin for (10 ng/mL) for 24 h, then rinsed three times with ice cold-PBS, fixed in 4% paraformaldehyde for 25 min at room temperature, washed, and endogenous peroxidase activity quenched with 75 mmol/L NH4Cl and 20 mmol/L glycine in PBS. Primary antibody was incubated at a 1:50 dilution in PBS for 1 h at room temperature. Antibody detection was performed using an HRP-AEC staining kit using anti-mouse biotinylated antibodies (R&D Systems) and counterstained with hematoxylin (Sigma).

Statistical analyses. Numerical data are expressed as means ± SD. Statistical differences between the means for the different groups were evaluated with Instat 4.0 (GraphPAD software) using one-way ANOVA with the level of significance at a P value of <0.05. Where indicated, a Krusal-Wallis test and Dunn's multiple comparisons tests were used with the level of significance set at a P value of <0.05.

Results

Expression of CXCR6 in human PCa. To explore whether CXCR6 plays a role in PCa development, high-density tissue microarrays were stained with an anti-human CXCR6 antibody from clinical samples obtained from a cohort of 48 patients. Representative

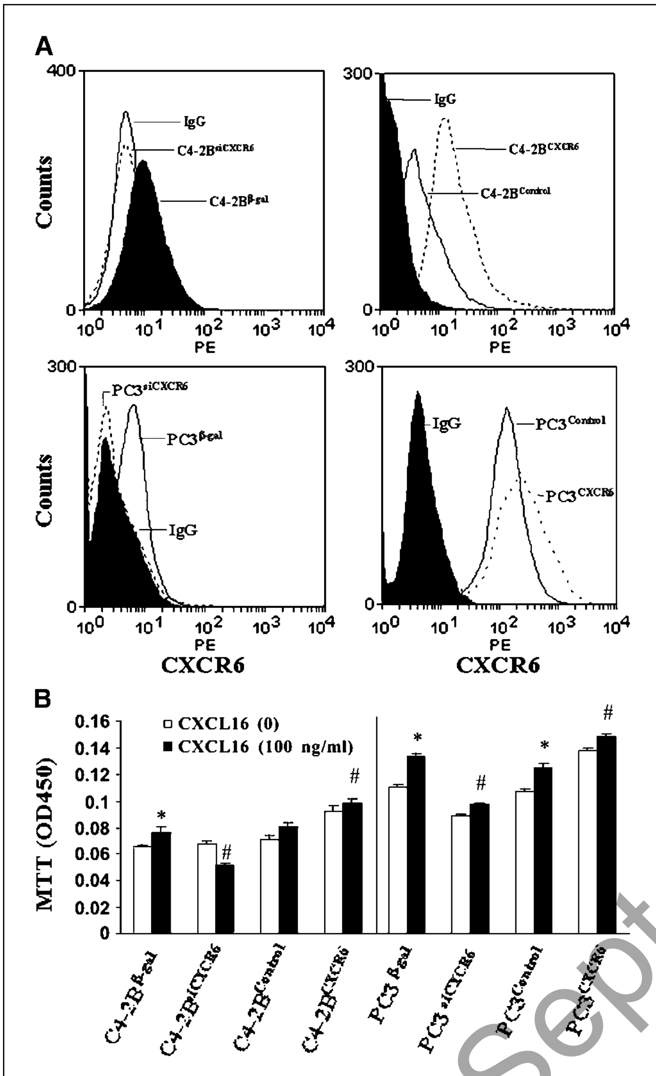

Figure 2. CXCR6 expression in PCa cells mediates cell invasion. *A,* FACS analysis of CXCR6 expression in transfected PCa cell lines. A mouse anti-human CXCR6 antibody was used to detect the expression of PCa cells overexpressing CXCR6 ($PC3^{CXCR6}$/$PC3^{Control}$ or $C4\text{-}2B^{CXCR6}$/$C4\text{-}2B^{Control}$) or in which CXCR6 expression is reduced using siRNA ($PC3^{siCXCR6}$/$PC3^{\beta\text{-}gal}$ or $C4\text{-}2B^{siCXCR6}$/$C4\text{-}2B^{\beta\text{-}gal}$). A β-gal sequence was incorporated into the siRNA as a vector control. *B,* CXCR6 regulates PCa cell invasion. PCa cell lines were placed in the top chamber of cell invasion plates containing a reconstituted extracellular matrix in serum-free RPMI, and CXCL16 (100 ng/mL) was added to the lower chambers. Invasion was determined at 48 h by MTT staining; *columns,* mean % invasion binding for $n = 5$; *bars,* SD. *, significant difference from nontreated controls; #, significant difference from invasion between alterations of CXCR6 expression with respective controls under CXCL16 stimulation (100 ng/mL; $P < 0.05$, ANOVA).

images are shown in Fig. 1*A*, demonstrating that CXCR6 expression increases as the tumor becomes more aggressive, whereas normal epithelium shows weak cytoplasmic staining (Fig. 1*A*). High-grade (Gleason score, 6–10) also showed strong cytoplasmic staining (Fig. 1*A*). Quantitative analysis confirmed that CXCR6 expression increases with increasing tumor grade (Fig. 1*B*). Thus, CXCR6 expression is correlated with tumor progression.

CXCR6 expression in PCa cells mediates cell invasion. To further explore the role of CXCR6 in PCa, lentiviral vectors were used to overexpress CXCR6 in PC3 and LNCaP C4-2B cells (termed $PC3^{CXCR6}$, $C4\text{-}2B^{CXCR6}$), or reduce CXCR6 expression by siRNA (termed $PC3^{siCXCR6}$, $C4\text{-}2B^{siCXCR6}$). After clone selection, individual clones were pooled and evaluated by FACS for CXCR6 expression (Fig. 2*A*).

Once individual tumor cells are bound to the endothelium, they must invade through the extracellular matrix to establish a metastasis. The ability of CXCR6 to regulate invasion was next studied using reconstituted extracellular matrices in porous culture chambers (Matrigel; Beckman Coulter Labware). Stimulation of the PCa cells with CXCL16 induced invasion of PC3 or C4-2B control cells, consistent with previous reports (5). Moreover, reduced expression of CXCR6 decreased the invasive abilities of PC3 or C4-2B cells in the presence of CXCL16 (Fig. 2*B*). As expected, PC3 or C4-2B cells overexpressing CXCR6 were more invasive in response to CXCL16 stimulation compared with control cells (Fig. 2*B*).

The effect of altered CXCR6 expression on cytokine secretion. Altered cytokine secretion is a hallmark of many cancers including PCa disease. The growth of new blood vessels (angiogenesis) within tumors is essential for tumor growth, maintenance, and metastasis (23, 24). Previously, we reported that the alterations in CXCR4 levels induced the secretion of IL-6, IL-8, tissue inhibitor of metalloproteinase 2, and VEGF by PCa cells (22). Based on the findings, we hypothesized that reduced CXCR6 expression is potentially linked to regulating expression of angiogenic growth factors. To test this possibility, antibody arrays targeting angiogenic cytokines were used. As shown in Fig. 3*A*, high levels of IL-6 and IL-8 were present in the CM derived from C4-2B control cells. However, the levels of IL-6 and IL-8 in medium collected from the CXCR6 siRNA-transfected C4-2B cells were significantly lower relative to control-treated cells (Fig. 3*A*). Similar reductions in IL-8 levels were also seen in PC3 CM after reductions in CXCR6 expression (Fig. 3*A*).

To further explore the proangiogenic signals regulated by CXCR6, CM derived from the various CXCR6 transfectants were analyzed by ELISA. As shown in Fig. 3*B*, siRNA targeting of CXCR6 expression in C4-2B and PC3 cells resulted in significant reductions in the levels of IL-8 compared with the control cells, consistent with our antibody array data. In contrast, IL-8 production in cells overexpressing CXCR6 was significantly enhanced (Fig. 3*B*). Likewise, IL-6 levels in the PCa transfectants generally followed a similar pattern of expression with the exception that overexpression of CXCR6 in PC3 cells did not alter the IL-6 levels produced (Fig. 3*B*).

To explore whether CXCR6 expression is biologically relevant to vascular recruitment by PCa cells, human endothelial cell sprout formation was used as *in vitro* assay measuring proangiogenic activity. Shown in Fig. 3*C*, little or no sprout formation occurred in the absence of external stimuli applied to endothelial cells alone *in vitro*. Coculture of the endothelial cells with either the CM derived from PC3 or C4-2B cells stimulated robust vascular sprout formation (Fig. 3*C*). Reduced expression of CXCR6 in both cells dramatically decreased blood vessel sprout formation (Fig. 3*C*). Overexpression of CXCR6 in C4-2B cells increased vessel formation relative to the respective control (Fig. 3*C*). Moreover, by adding a CXCR6-blocking antibody decreased the effects of the CM relative to an IgG antibody control. This suggests that CXCL16 and CXCR6 activate an autocrine/paracrine loop in human endothelial cells and PCa cells, which is likely to play a role in proangiogenic activity that may contribute to PCa development (Supplementary Fig. S2).

Effects of CXCR6 expression on tumor growth and angiogenesis *in vivo*. To confirm that CXCR6 plays a role in tumor growth, SCID mice were implanted s.c. with cells engineered

to express altered levels of CXCR6. As shown in Fig. 4*A*, tumors generated from C4-2B cells overexpressing CXCR6 were significantly larger than tumors generated by the transfected control group (257.1 ± 80.5 mg versus 665.3 ± 65.3 mg). In parallel, tumor growth was dramatically suppressed in tumors established from cells in which CXCR6 expression was decreased by transfection of lentivirus-siRNA vector relative to controls (336.5 ± 62.5 mg versus 165.6 ± 60.3 mg; Fig. 4*A*).

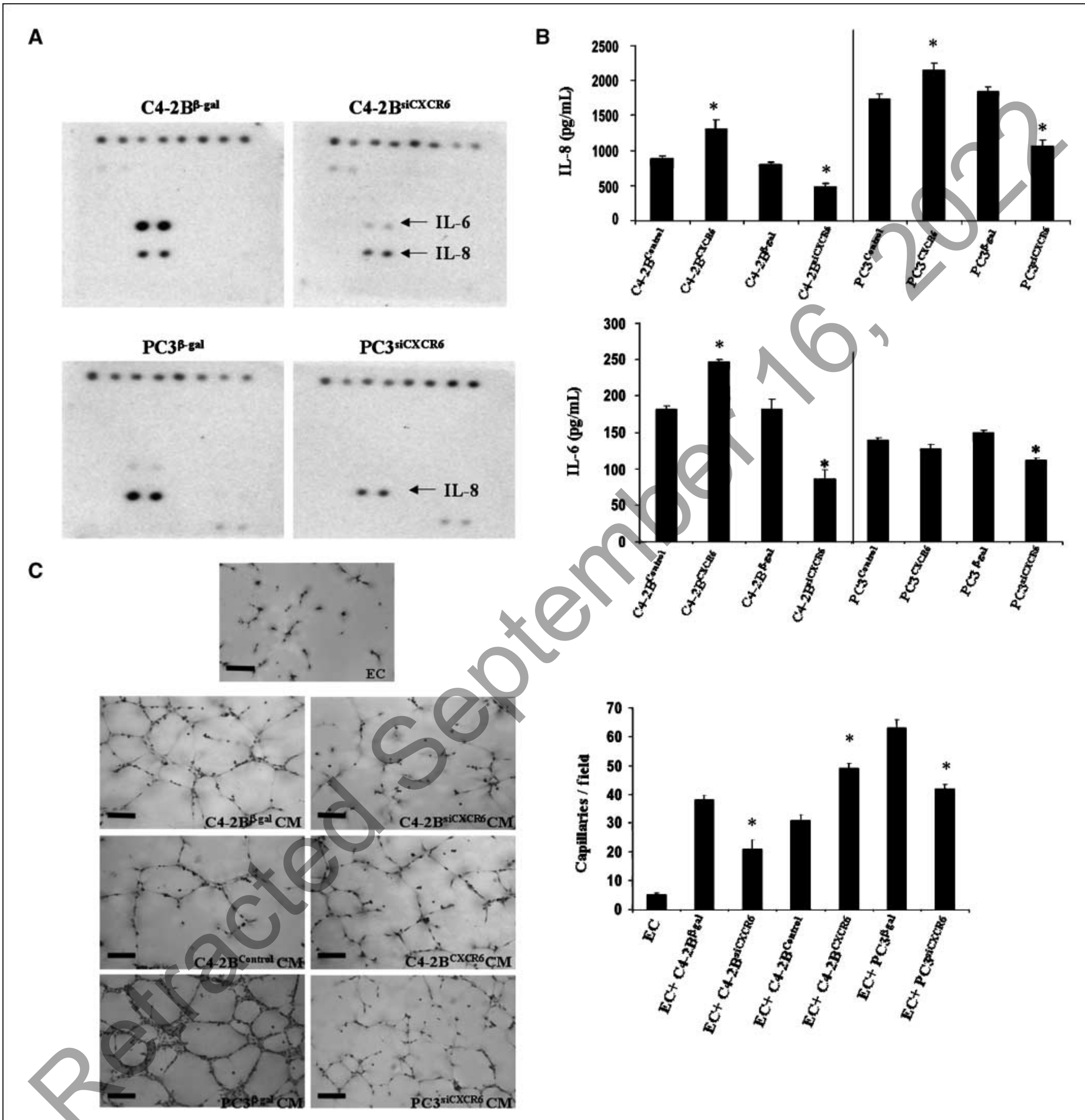

Figure 3. CXCR6 expression regulates IL-8 and IL-6 secretion. *A,* detection of cytokines for angiogenesis in a cytokine array. Detection of cytokines from CM derived from PC-3 and C4-2B cells expressing reduced CXCR6 protein and their respective control cells. The CM was incubated with cytokine array membranes. The membranes were then incubated with a combination of multiple biotin-conjugated anticytokine and HRP-conjugated streptavidin. The signals were visualized by chemoluminescense. The data indicates alterations in IL-6 and IL-8 expression, after reduced CXCR6 expression. *B,* CXCR6 regulates secretion of IL-6 and IL-8 by PCa. IL-6 and IL-8 levels were evaluated by ELISA for PCa cells with altered expression of CXCR6 at 48 h. *Columns,* mean for triplicate determinations and normalized against total protein; *bars,* SD. *, significant difference from respective controls ($P < 0.05$, ANOVA). $n = 6$ in groups. *C,* effect of PCa expression of CXCR6 on blood vessel formation. HDMECs were plated in growth factor–reduced Matrigel in the presence or absence of the CM from PCa cells as a functional *in vitro* assay of blood vessel formation. After 24 h, the cultures were fixed and stained. As a negative control, only HDMECs were plated. Vessel sprout formation was quantified by direct microscopic counting. Original magnification, ×20; *black bars,* 100 μmol/L. *Columns,* mean for triplicate determinations; *bars,* SD. *, significant difference from controls ($P < 0.05$, ANOVA).

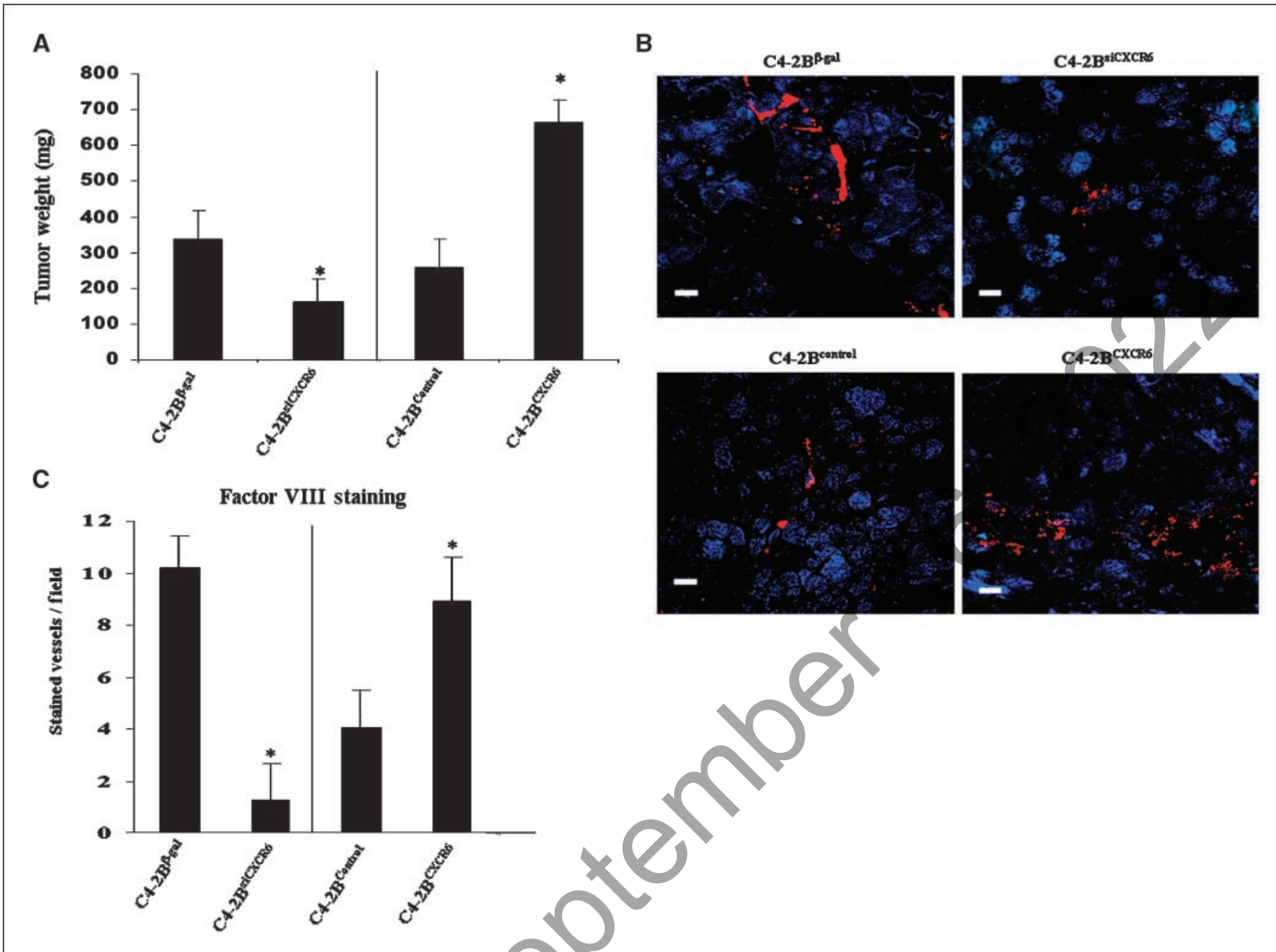

Figure 4. Effects of CXCR6 expression on tumor growth and angiogenesis *in vivo. A,* effect of CXCR6 expression on tumor weight. NOD/SCID mice were implanted s.c. with 1×10^6 C4-2B cells expressing various levels of CXCR6. Tumor weight was measured at sacrifice. *Columns,* mean for triplicate determinations of $n = 8$ in groups; *bars,* SD. *, significant difference from the controls ($P < 0.05$, ANOVA). *B,* histologic evaluation of microvessel growth in tumors with altered CXCR6 levels. The numbers of stained microvessels were blindly counted in 10 random fields per implant at a final magnification of ×630. Five tumor implants were analyzed per condition by immunostaining in tumor frozen slides for human von Willebrand factor (28 mg/mL anti-rabbit IgG). Nuclei were identified by DAPI. All images were generated on Zeiss LSM 510 meta confocal laser scanning microscope. *C,* quantification of microvessel formation in tumors with altered CXCR6 levels. The numbers of stained microvessels were blindly evaluated in 10 random fields per implant at ×200 magnifications. *, significant difference from the controls ($P < 0.05$, ANOVA).

To address directly whether CXCR6 was able to play a role in tumor angiogenesis, the tumors were stained with an antibody to factor VIII, a specific marker for vascular endothelial cells. Overexpression of CXCR6 in C4-2B cells resulted in more abundant blood vessel formation than in tumors generated by the control transfected cells (Fig. 4*B*). In contrast, fewer and smaller blood vessels were seen when the expression of CXCR6 was reduced compared with the respective control (10.2 ± 1.2 versus 2.3 ± 1.4 per high-powered field; Fig. 4*C*). Similar results were observed in $PC3^{siCXCR6}$ cells (data not shown).

Activation of AKT/mTOR/S6K signaling by CXCL16 in PCa cells. Previously, we and others have shown that activation of CXCR4 by CXCL12 results in activation of extracellular signal-regulated kinase (ERK) and AKT pathways in PCa cells (8, 9). Activation of ERK and AKT after CXCL12 stimulation results in alterations in several angiogenic factors and MMP production known to regulate PCa angiogenesis, invasion, and progression (8, 22). Next, we determine which pathway is involved in activation of CXCR6 by CXCL16 stimulation. As shown in Fig. 5*A*, stimulation of CXCL16 induced intense phosphorylation of Akt in C4-2B control cells, which peaked by 45 minutes. In this case, reduced phosphorylation of Akt was observed after reduced CXCR6 expression as early as 10 minutes. AKT activation is known to trigger many downstream components of the mTOR pathway including p70S6K and 4E-BP1. Here, CXCL16 stimulation activated p70S6K and 4E-BP1 in C4-2B control cells, in which the peak expression of phosphorylation of p70S6K was observed at 30 and 45 minutes and, for 4E-BP1, were seen at 10 and 30 minutes (Fig. 5*A*). In contrast, phosphorylation of p70S6K and 4E-BP1 was significantly reduced in C4-2B cells with reduced CXCR6 expression (Fig. 5*A*). Moreover, addition of the mTOR inhibitor rapamycin selectively inhibited CXCL16-induced activation of p70S6K and 4E-BP1 in C4-2B cells in a dose-dependent manner. Similar findings were also observed in PC3 cells (Fig. 5*B*). Taken together, these data suggest that CXCL16 stimulation through CXCR6 activates the AKT/mTOR/p70S6K pathway in PCa cells.

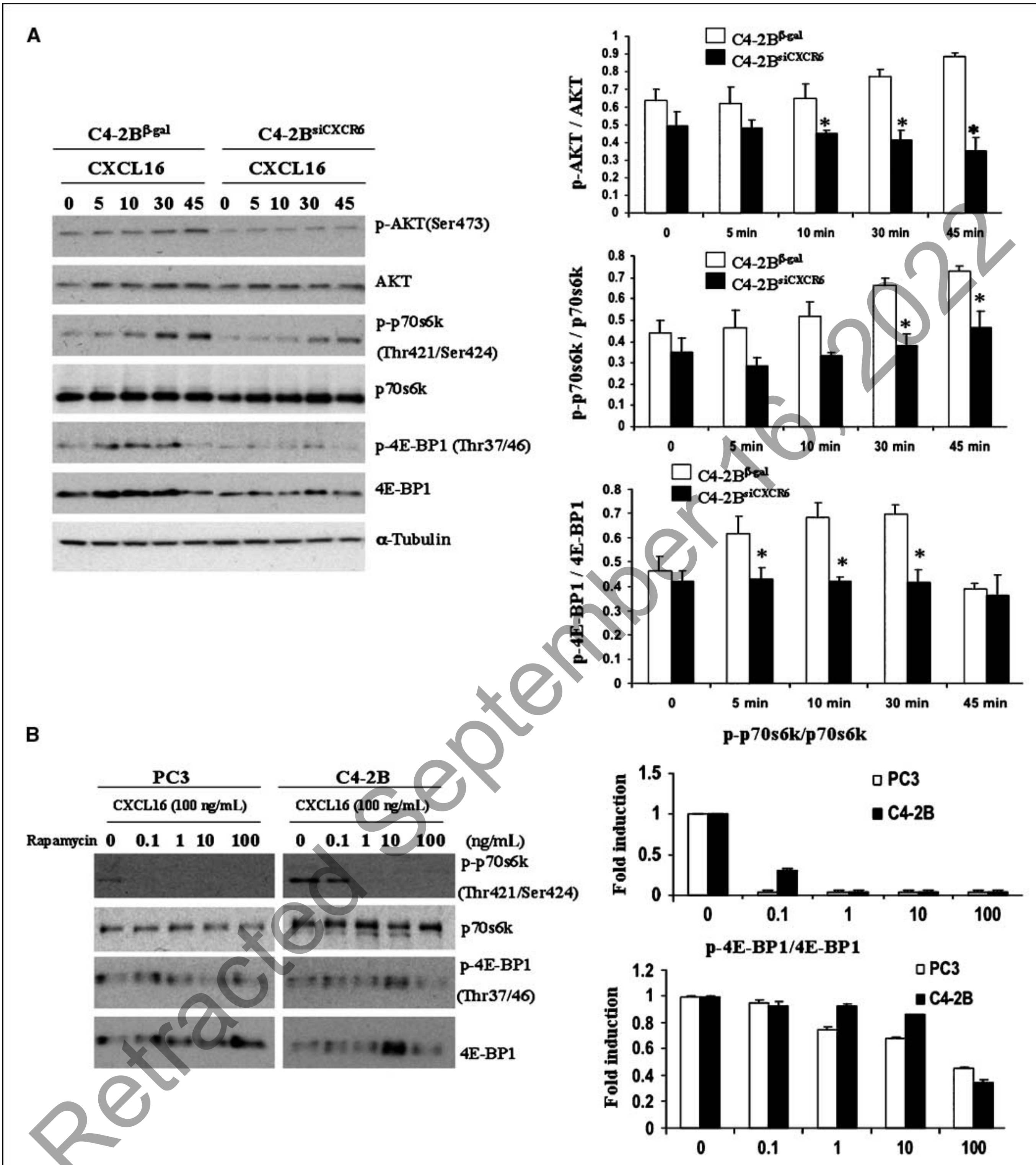

Figure 5. CXCR6 mediates CXCL16-induced activation of the AKT/mTOR signaling pathway. *A,* evaluation of the effect of CXCR6 on of AKT/mTOR signaling. After a 24-h serum withdrawal, PCa cells were stimulated with 100 ng/mL CXCL16. Whole cell lysates were separated on SDS-PAGE and immunoblotted with antibodies to phospho-AKT (Ser473), p70S6K (Thr421/Ser424), and p4E-BP1 (Thr37/46), and total AKT, p70S6K (S6K), and 4E-BP1. The blots were stripped and reblotted with antibodies against total AKT, p70S6K (S6K), and 4E-BP1 respectively (*left*). Quantitative densitometry was used for direct comparison (*right*). *Columns,* mean for triplicate determinations; *bars,* SD. *, significant difference from the controls ($P < 0.05$, Krusal-Wallis test, and Dunn's multiple comparisons test). *B,* rapamycin inhibits CXCL16-induced activation of the mTOR pathway. Inhibitors of mTOR (rapamycin, 0–100 ng/mL) were added 30 min before initiation of chemokine CXCL16 stimulation. Akt, p70S6K, and 4E-BP1 phosphorylation in response to CXCL16 stimulation at 30 min was assessed in the presence or absence of rapamycin. Constitutively phosphorylated p70S6K and phosphorylated 4E-BP1 in PC3 and C4-2B cells are inhibited even at low concentrations of rapamycin (*left*). The relative fold decrease in phosphorlation is shown as signal intensity overloading their total protein expression (*right*). *Columns,* mean of two independent experiments; *bars,* SD.

The role of the mTOR pathway in CXCL16-promoted metastatic cell properties, cell growth, and secretion of cytokines. As our previous studies suggest that CXCL16 through CXCR6 is able to regulate several activities associated with metastasis, we next investigated how mTOR signaling regulates PCa growth and metastasis. First, we explored whether mTOR signaling inhibitor alters expression of MMPs and CD44 in PCa cells, as critical molecules activated for invasion. As shown in Supplementary Fig. S3, treatment with an mTOR inhibitor, rapamycin (10 ng/mL), did not significantly alter MMPs and CD44 expression in PCa cells relative to the untreated control. The results suggest that the mTOR signaling inhibitor rapamycin did not alter the intrinsic expression of MMPs (MMP-2, 3, and 9) and CD44 in PCa cells. Then, we further explored whether CXCL16 stimulation induced the expression of MMPs and CD44. The results indicated that expression of MMP-2 (Fig. 6*A*) and MMP-9 (data not presented) were not regulated by CXCL16, nor did treatment with the mTOR inhibitor rapamycin alter their expression by the PCa cells. Expression of MMP-3 was however increased by stimulation with CXCL16 by 24h in PC3 cells and by 48 hours for C4-2B cells. Here, rapamycin inhibited the MMP-3 expression induced by CXCL16. Intriguingly, CXCL16 was able to induce expression of CD44 in PC3 cells but not in C4-2B cells. The effect was also significantly inhibited by rapamycin (Fig. 6*A*).

Taken together, the findings suggest that CXCL16 may promote the expression of several activities necessary for metastasis through the mTOR pathway. Subsequent studies examined the effects of rapamycin on CXCL16-mediated invasion. As shown in Fig. 6*B*, induction of invasion by CXCL16 in PC3 and C4-2B cells was blocked by rapamycin in a concentration-dependent manner. Rapamycin also perturbed CXCL16-induced growth of PC3 and C4-2B cells by Ki-67 staining (Fig. 6*C*), a proliferation marker.

As previously noted, CXCR6 expression is correlated with the expression of proangiogenic factors IL-8 and IL-6 (Fig. 3*B*). The possible mechanism was further elucidated after blockade of the mTOR pathway with rapamycin. We observed that the secretion of both IL-8 and VEGF stimulated by CXCL16 was significantly reduced by rapamycin (Fig. 6*D*). These results suggest that blocking the mTOR pathway reduced CXCL16-induced secretion of IL-8 and VEGF cytokines associated with proangiogenic activity.

Discussion

Growing evidence suggests that chemokines and their receptors play a central role in the progression of multiple tumors. Our previous work has shown that CXCL12 (SDF-1) and its receptor (CXCR4) are critical elements in growth and metastasis of PCa to tissues that produce large quantities of CXCL12 (8, 9). We have also shown that a second CXCL12 receptor, CXCR7/RDC1, seems to play a similar role in PCa metastasis (10). However, not all of the invasive activities could be neutralized by inhibiting the activity of these molecules. Accordingly, we explored whether other members of the chemokine family participated in the metastatic cascade of PCa. CXCL16 is a type I membrane protein containing a non-ELR motif–containing CXC chemokine domain in its extracellular region. The cognate receptor for CXCL16 has been identified as CXCR6, a receptor previously shown to be a coreceptor for HIV entry (25, 26). Several groups indicated that CXCL16/CXCR6 signaling correlates with liver-specific homing (20) and lung-specific homing (25, 26) in the event of inflammation. Previous studies have shown that CXCL16 signaling through CXCR6 may contribute to PCa progression by serving as a proliferative signal and as a regulator of invasion (5, 15). However, the mechanism of this chemokine axis involved in PCa progression has not been elucidated. In this investigation, we found that CXCR6 expression is correlated with PCa aggressiveness. A similar correlation has been shown in patients with gliomas (23), nasopharyngeal tumors (24), rectal cancer (14), colorectal cancer (27), and melanomas (28), suggesting that CXCR6 expression is important for invasion and metastasis of multiple tumors.

CXCR6 is a member of the seven transmembrane G protein–coupled receptor family, many of whose members signal through the AKT/mTOR pathway. AKT/mTOR has been shown to play a central role in the development of PCa by regulating cell growth and cell cycle progression (29–31). Upon activation, mTOR, a serine/threonine kinase, is responsible for phosphorylation and activation of its two major downstream components, p70S6K and eIF4E-binding protein 1 (4E-BP1). Phosphorylation of p70S6K facilitates the translation of ribosomal proteins (29), and, also, phosphorylation of 4E-BP1 regulates cap-dependent translation by enabling the formation of an active eIF4E complex, all of which are important events in the regulation of mRNA translation (29). Here, we observed that CXCL16 stimulation through the CXCR6/AKT/mTOR pathway induced the activation of p70S6K and 4E-BP1, which were blocked by mTOR inhibitor rapamycin. Furthermore, rapamycin not only inhibited CXCL16-induced proliferation, invasion, and expression of CD44 and MMP3, but also reduced secretion of IL-8 and VEGF, associated with proangiogenic activity in PCa cells. CD44 is a multifunctional protein involved in cell adhesion and signaling. The role of CD44 in PCa development and progression is controversial, with studies showing both tumor-promoting and tumor-inhibiting effects (32). CD44 has also been found to play a role in the metastatic behavior of tumor progenitor/PCa stem cell homing (32). Similar observations have been found in head and neck cancer (33), pancreatic cancer (34), and PCa stem cells (35). MMPs are a multifunctional family of proteins, involved in the degradation of extracellular matrix and basement membrane barriers (36–38). Members of the family have been implicated in the promotion of tumor growth, angiogenesis, invasion, and metastasis (27, 39), in which elevated MMP levels are associated with poor prognosis (40). In this study, we found that CXCL16 induced MMP-3 expression but not MMP-2 and MMP-9. Each of these activities was inhibited by rapamycin. The findings suggest that CXCL16 activates molecules necessary for metastasis through the mTOR pathway.

In addition to regulating cell growth and invasion, CXCR6 seems to regulate blood vessel formation by PCa cells or endothelial cells by an autocrine/paracrine loop. It was further observed that both IL-8 and IL-6 levels were altered in response to changes in CXCR6 expression. These findings are in keeping with the number of blood vessels formed by the tumors *in vivo*. IL-8 and IL-6 have been shown to be important factors involved in the development of tumor blood supply in the progression of solid tumors after activation of ERK or AKT pathways (41). Our results suggest that CXCR6 enhances tumor growth through activation of AKT pathways to induce angiogenesis. This was confirmed by blocking the AKT/mTOR pathway, which resulted in reduced secretion of IL-8 and VEGF after CXCL16 stimulation. In fact, these findings are similar to results that we previously reported on the role of CXC12/CXCR4 and CXCR7 (10). Notably, cross-talk between these receptors (CXCL12/CXCR4 and CXCL16/CXCR6) is likely to

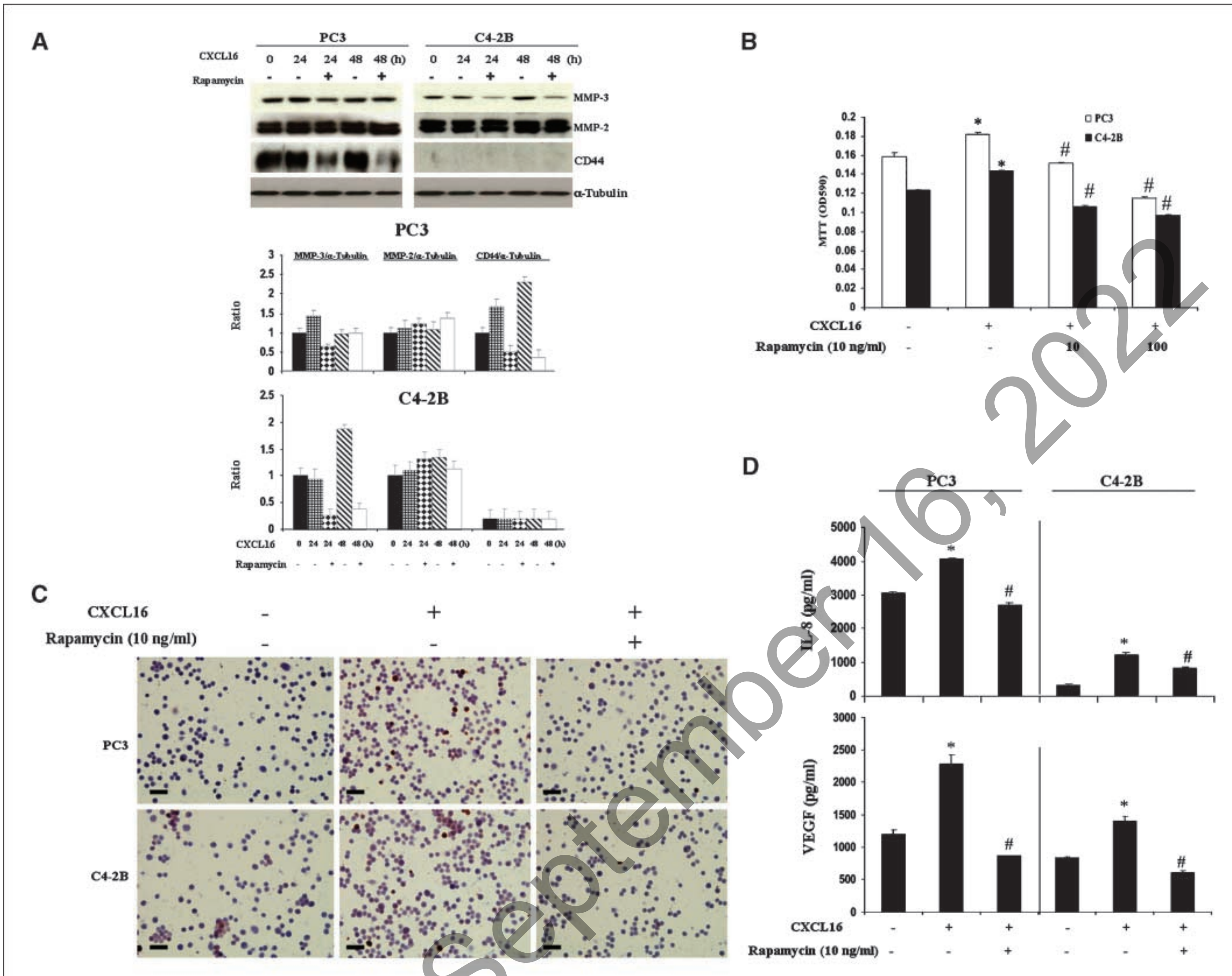

Figure 6. Blocking mTOR signaling inhibits expression of MMP-3, CD44 proliferation, and invasion stimulated by CXCL16 in PCa cells. *A,* rapamycin inhibits CXCL16-induced MMP-3 and CD44 expression. Expression of MMPs and CD44 in PC3 and C4-2B cells stimulated with or without CXCL16 for 24 or 48 h was assayed by Western blot analysis. Cells lysates were resolved by SDS-PAGE and immunoblotted with antibodies to the indicated MMPs and CD44. The blots were stripped and reblotted to ensure proper loading. CXCL16-promoted MMP-3 and CD44 expression was clearly inhibited by treatment with the mTOR inhibitor rapamycin (10 ng/mL). The relative fold changes in expression are shown as signal intensity relative to α-tubulin protein expression (*right*). Columns, mean of two independent experiments; *bars,* SD. *B,* rapamycin inhibits CXCL16-induced PCa cell invasion. PC3 and C4-2B cells were examined for cell invasion to CXCL16 using Transwell plates. Chemotactic responses of PC3 and C4-2B cells to CXCL16 were dose-dependently observed. The effects were inhibited by rapamycin. *Columns,* mean number of migrated cells per field from a representative experiment performed in triplicate; *bars,* SD. *, significant difference from CXCL16 stimulation (100 ng/mL); #, significant from rapamycin treatment ($P < 0.05$, ANOVA). $n = 4$ in groups. *C,* rapamycin inhibits CXCL16-induced PCa cell growth. Cytospin preparations of PC3 and C4-2B cells were stained with antibody to Ki-67, a proliferation marker. Hematoxylin was used for counterstaining. Representative immunohistochemical staining of Ki-67 (*brown*, nuclear) of the indicated cell cultures is shown. Original magnification, ×40; *black bars,* 50 μmol/L. *D,* rapamycin inhibits CXCL16-induced secretion of IL-8 and VEGF. IL-8 and VEGF levels were tested by ELISA in supernatants from rapamycin-treated PCa cells. *Columns,* mean; *bars,* SD for triplicate determinations and normalized against total protein. *, significant difference from CXCL16 stimulation (100 ng/mL); #, significant from rapamycin treatment ($P < 0.05$, ANOVA). $n = 4$ in groups.

play an important role in tumor development or progression (Supplementary Fig. S1).

The mTOR signaling cascade is critical for the growth and survival of malignant hematopoietic and solid tumor cells (40). Extensive work conducted over the past decade has firmly established the relevance of this pathway in the control of important cellular responses, and has documented its aberrant/abnormal activation in several malignancies (42). Currently, the mTOR inhibitor rapamycin and its derivatives, such as CCI-779, RAD001, and AP23573, are being evaluated in cancer clinical trials including for hematologic malignancies, renal cancer, breast cancer, lymphoma, glioblastoma, sarcoma, and several solid cancers (43, 44). To our knowledge, this represents the first report describing the contribution of CXCR6 to activating the AKT/mTOR pathway in PCa development. It is important to note that because the mTOR cascade cross-talks with other pathways, combinations of mTOR inhibitors with other therapeutic agents have produced synergistic effects on inhibiting tumor growth in experimental models and in some clinical trials (45, 46). The immediate challenge is therefore to determine how mTOR inhibitors can be applied in a tumor-specific manner to minimize adverse effects by blocking a pathway with broad biological significance.

In conclusion, our results suggest that CXCR6 expression is associated with invasive growth and angiogenic activities of PCa cells. Furthermore, we show that blocking the CXCR6/AKT/mTOR signaling pathway induces antimetastatic properties in PCa cells, which might be beneficial in development of a more effective therapeutic strategy for PCa.

Disclosure of Potential Conflicts of Interest

No potential conflicts of interest were disclosed.

Acknowledgments

Received 7/21/2008; revised 9/5/2008; accepted 9/23/2008.

Grant support: Department of Defense DOD PC051407 fellowship award (J. Wang), National Cancer Institute PO1 award CA93900 (R.S. Taichman), and Department of Defense awards PC061231 (J. Zhang), PC060857, and PC073952 (R.S. Taichman). A.E. Koch is supported by NIH grants AI40987, AR48267, the Office of Research and Development, Medical Research Service, Dept. of Veteran's Affairs, and funds from the Frederick G.L. Huetwell and William D. Robinson, MD Professorship in Rheumatology.

The costs of publication of this article were defrayed in part by the payment of page charges. This article must therefore be hereby marked *advertisement* in accordance with 18 U.S.C. Section 1734 solely to indicate this fact.

References

1. Mundy GR. Metastasis to bone: causes, consequences and therapeutic opportunities. Nat Rev Cancer 2002;2:584–93.
2. Roodman GD. Mechanisms of bone metastasis. N Engl J Med 2004;350:1655–64.
3. Wang J, Loberg R, Taichman RS. The pivotal role of CXCL12 (SDF-1)/CXCR4 axis in bone metastasis. Cancer Metastasis Rev 2006;25:573–87.
4. Kollet O, Shivtiel S, Chen YQ, et al. HGF, SDF-1, and MMP-9 are involved in stress-induced human CD34+ stem cell recruitment to the liver. J Clin Invest 2003;112:160–9.
5. Lu Y, Wang J, Xu Y, et al. CXCL16 functions as a novel chemotactic factor for prostate cancer cells *in vitro*. Mol Cancer Res 2008;6:546–54.
6. Muller A, Homey B, Soto H, et al. Involvement of chemokine receptors in breast cancer metastasis. Nature 2001;410:50–6.
7. Taichman RS, Cooper C, Keller ET, et al. Use of the stromal cell-derived factor-1/CXCR4 pathway in prostate cancer metastasis to bone. Cancer Res 2002;62:1832–7.
8. Darash-Yahana M, Pikarsky E, Abramovitch R, et al. Role of high expression levels of CXCR4 in tumor growth, vascularization, and metastasis. FASEB J 2004;18:1240–2.
9. Sun YX, Wang J, Shelburne CE, et al. Expression of CXCR4 and CXCL12 (SDF-1) in human prostate cancers (PCa) *in vivo*. J Cell Biochem 2003;89:462–73.
10. Wang J, Shiozawa Y, Wang J, et al. The role of CXCR7/RDC1 as a chemokine receptor for CXCL12/SDF-1 in prostate cancer. J Biol Chem 2008;283:4283–94.
11. Tabata S, Kadowaki N, Kitawaki T, et al. Distribution and kinetics of SR-PSOX/CXCL16 and CXCR6 expression on human dendritic cell subsets and CD4+ T cells. J Leukoc Biol 2005;77:777–86.
12. Volin MV, Woods JM, Amin MA, et al. Fractalkine: a novel angiogenic chemokine in rheumatoid arthritis. Am J Pathol 2001;159:1521–30.
13. Hanamoto H, Nakayama T, Miyazato H, et al. Expression of CCL28 by Reed-Sternberg cells defines a major subtype of classical Hodgkin's disease with frequent infiltration of eosinophils and/or plasma cells. Am J Pathol 2004;164:997–1006.
14. Wagsater D, Dimberg J. Expression of chemokine receptor CXCR6 in human colorectal adenocarcinomas. Anticancer Res 2004;24:3711–4.
15. Chandrasekar B, Bysani S, Mummidi S. CXCL16 signals via Gi, phosphatidylinositol 3-kinase, Akt, I κ B kinase, and nuclear factor-κ B and induces cell-cell adhesion and aortic smooth muscle cell proliferation. J Biol Chem 2004;279:3188–96.
16. Abel S, Hundhausen C, Mentlein R, et al. The transmembrane CXC-chemokine ligand 16 is induced by IFN-γ and TNF-α and shed by the activity of the disintegrin-like metalloproteinase ADAM10. J Immunol 2004;172:6362–72.
17. Gough PJ, Garton KJ, Wille PT, et al. A disintegrin and metalloproteinase 10-mediated cleavage and shedding regulates the cell surface expression of CXC chemokine ligand 16. J Immunol 2004;172:3678–85.
18. Wilbanks A, Zondlo SC, Murphy K, et al. Expression cloning of the STRL33/BONZO/TYMSTRligand reveals elements of CC, CXC, and CX3C chemokines. J Immunol 2001;166:5145–54.
19. Nakayama T, Hieshima K, Izawa D, et al. Cutting edge: profile of chemokine receptor expression on human plasma cells accounts for their efficient recruitment to target tissues. J Immunol 2003;170:1136–40.
20. Kim CH, Kunkel EJ, Boisvert J, et al. Bonzo/CXCR6 expression defines type 1-polarized T-cell subsets with extralymphoid tissue homing potential. J Clin Invest 2001;107:595–601.
21. Deng HK, Unutmaz D, KewalRamani VN, et al. Expression cloning of new receptors used by simian and human immunodeficiency viruses. Nature 1997;388:296–300.
22. Wang J, Wang J, Sun Y, et al. Diverse signaling pathways through the SDF-1/CXCR4 chemokine axis in prostate cancer cell lines leads to altered patterns of cytokine secretion and angiogenesis. Cell Signal 2005;17:1578–92.
23. Ludwig A, Schulte A, Schnack C, et al. Enhanced expression and shedding of the transmembrane chemokine CXCL16 by reactive astrocytes and glioma cells. J Neurochem 2005;93:1293–303.
24. Ou DL, Chen CL, Lin SB, et al. Chemokine receptor expression profiles in nasopharyngeal carcinoma and their association with metastasis and radiotherapy. J Pathol 2006;210:363–73.
25. Agostini C, Cabrelle A, Calabrese F, et al. Role for CXCR6 and its ligand CXCL16 in the pathogenesis of T-cell alveolitis in sarcoidosis. Am J Respir Crit Care Med 2005;172:1290–8.
26. Ruth JH, Haas CS, Park CC, et al. CXCL16-mediated cell recruitment to rheumatoid arthritis synovial tissue and murine lymph nodes is dependent upon the MAPK pathway. Arthritis Rheum 2006;54:765–78.
27. Okada N, Ishida H, Murata N, et al. Matrix metalloproteinase-2 and -9 in bile as a marker of liver metastasis in colorectal cancer. Biochem Biophys Res Commun 2001;288:212–6.
28. Seidl H, Richtig E, Tilz H, et al. Profiles of chemokine receptors in melanocytic lesions: *de novo* expression of CXCR6 in melanoma. Hum Pathol 2007;38:768–80.
29. Kaur S, Sassano A, Dolniak B, et al. Role of the Akt pathway in mRNA translation of interferon-stimulated genes. Proc Natl Acad Sci U S A 2008;105:4808–13.
30. Majumder PK, Sellers WR. Akt-regulated pathways in prostate cancer. Oncogene 2005;24:7465–74.
31. Sodhi A, Chaisuparat R, Hu J, et al. The TSC2/mTOR pathway drives endothelial cell transformation induced by the Kaposi's sarcoma-associated herpesvirus G protein-coupled receptor. Cancer Cell 2006;10:133–43.
32. Patrawala L, Calhoun T, Schneider-Broussard R, et al. Highly purified CD44+ prostate cancer cells from xenograft human tumors are enriched in tumorigenic and metastatic progenitor cells. Oncogene 2006;25:1696–708.
33. Prince ME, Sivanandan R, Kaczorowski A, et al. Identification of a subpopulation of cells with cancer stem cell properties in head and neck squamous cell carcinoma. Proc Natl Acad Sci U S A 2007;104:973–8.
34. Galkina E, Harry BL, Ludwig A, et al. CXCR6 promotes atherosclerosis by supporting T-cell homing, interferon-γ production, and macrophage accumulation in the aortic wall. Circulation 2007;116:1801–11.
35. Collins AT, Berry PA, Hyde C, et al. Prospective identification of tumorigenic prostate cancer stem cells. Cancer Res 2005;65:10946–51.
36. Curran S, Murray GI. Matrix metalloproteinases in tumour invasion and metastasis. J Pathol 1999;189:300–8.
37. de Vicente JC, Lequerica-Fernandez P, Lopez-Arranz JS, et al. Expression of matrix metalloproteinase-9 in high-grade salivary gland carcinomas is associated with their metastatic potential. Laryngoscope 2008;118:247–51.
38. Kahari VM, Saarialho-Kere U. Matrix metalloproteinases and their inhibitors in tumour growth and invasion. Ann Med 1999;31:34–45.
39. Acuff HB, Carter KJ, Fingleton B, et al. Matrix metalloproteinase-9 from bone marrow-derived cells contributes to survival but not growth of tumor cells in the lung microenvironment. Cancer Res 2006;66:259–66.
40. Bjornland K, Flatmark K, Pettersen S, et al. Matrix metalloproteinases participate in osteosarcoma invasion. J Surg Res 2005;127:151–6.
41. Jubb AM, Hurwitz HI, Bai W, et al. Impact of vascular endothelial growth factor-A expression, thrombospondin-2 expression, and microvessel density on the treatment effect of bevacizumab in metastatic colorectal cancer. J Clin Oncol 2006;24:217–27.
42. Dutcher JP. Mammalian target of rapamycin (mTOR) Inhibitors. Curr Oncol Rep 2004;6:111–5.
43. Easton JB, Houghton PJ. Therapeutic potential of target of rapamycin inhibitors. Expert Opin Ther Targets 2004;8:551–64.
44. Vignot S, Faivre S, Aguirre D, et al. mTOR-targeted therapy of cancer with rapamycin derivatives. Ann Oncol 2005;16:525–37.
45. Choo AY, Blenis J. TORgeting oncogene addiction for cancer therapy. Cancer Cell 2006;9:77–9.
46. Rubio-Viqueira B, Hidalgo M. Targeting mTOR for cancer treatment. Curr Opin Investig Drugs 2006;7:501–12.